LARGE-AMPLITUDE FORCED VIBRATIONS OF THIN SHALLOW SPHERICAL SHELLS : REDUCED-ORDER MODELS AT RESONANCE AND MODE COUPLING

Olivier Thomas[♭], Cyril Touzé[♯]

[♭]CNAM-LMSSC, 2 rue Conté, 75003 Paris, France, *olivier.thomas@cnam.fr*
[♯]ENSTA-UME, Chemin de la Hunière, 91761 Palaiseau Cedex, France, *cyril.touze@ensta.fr*

Keywords: shallow shells, internal resonance, nonlinear modes, reduced order model, real normal form.

Abstract: *This work is devoted to the study of non-linear large amplitude vibrations of thin spherical shells. A specific mode coupling due to a 1:1:2 internal resonance between an axisymmetric mode and two companion asymmetric modes is especially addressed. The aim of the study is to compare two reduced-order models and a set of experiments. The first model (model A) is obtained by projecting the non-linear partial differential equations onto the eigenmodes basis and then by retaining only (i) the three oscillators associated to the modes involved in the internal resonance (ii) the quadratic terms. Secondly, a more refined model (model B) using three non-linear modes computed asymptotically with a real normal form enables to include the effects of the cubic terms and the modes not primary involved in the internal resonance. Resonance curves, showing the amplitude of the modes as functions of the driving frequency and stemming from both models and the experiments, are discussed. It is shown that model B brings features that are observed experimentally and not predicted by model A.*

1 INTRODUCTION

Structures with a thin geometry, like beams, arches, plates and shells, can exhibit large amplitude flexural vibrations, whose magnitude is comparable to the order of their thickness. In those cases, typical non-linear behaviors can be observed, such as jump phenomena and energy exchanges between modal configurations and a linear prediction model is not sufficient [1]. This article addresses non-linear large amplitude vibrations of thin spherical shells and is specifically devoted to a particular mode coupling due to a 1:1:2 internal resonance between an axisymmetric mode and two companion asymmetric modes.

The 1:1:2 internal resonance involves in our study a modal interaction between two companion asymmetric modes, which have nearly equal natural frequencies $f_1 \simeq f_2$ (thus being in one-to-one (1:1) internal resonance) and one axisymmetric mode, whose natural frequency f_3 is close to twice the ones of the asymmetric companion modes (all three being in 1:1:2 internal resonance, $f_1 \simeq f_2 \simeq f_3/2$). The spherical shell is driven by a simple-harmonic force at its center, in the vicinity of the resonance of the axisymmetric mode, and the boundary conditions are free at the edge. A transfer of energy toward the asymmetric companion modes is observed, those modes oscillating at half the driving frequency, thus creating a subharmonic in the shell response.

In a previous work of the authors [2], a theoretical model of a spherical shell subjected to large amplitude asymmetric non-linear vibrations has been derived, using the analog for thin shallow shells of von Kármán equations for plates. These PDE have been discretized by projection onto the eigenmodes basis of the associated linear problem. Then, a simple reduced order model of the 1:1:2 internal resonance (model A) has been obtained by retaining only the three oscillators associated to the modes involved in the internal resonance and the quadratic terms. The results of this model have been compared to experimental data in [3]. An excellent qualitative agreement was found. However, some quantitative discrepancies were noticed. Two major explanations have been formulated. Firstly, the imperfections of the geometry of the shell, slight in appearance, seem to have a major effect on the vibratory response of the shell. As an example, the theoretical value of the axisymmetric mode natural frequency is 386 Hz whereas its measured value is 225 Hz. Secondly, it was found that the influence of the cubic terms arising from the geometrical non-linearities seem to be important.

In this article, an improved reduced-order model (model B) is proposed and compared to the above mentioned model A. It is based on non-linear normal modes (NNM), defined as invariant manifold of the phase

space and computed by an asymptotic development of the real normal form of the problem. This method has been described for the conservative case in [4] and successfully applied to predict the correct trend of non-linearity of the modes of a spherical shell in [5]. Modal damping has recently been taken into account in [6]. Model B then consists of describing the dynamics by the three NNMs corresponding to the three modes involved in the 1:1:2 internal resonance. It is shown that in spite of its small size (3 NNMs), model B offers results closer to the experiments than the ones obtained in [2] and it recovers specific solutions that could not be predicted by model A, such as amplitude-modulated solutions.

2 THEORETICAL MODELS

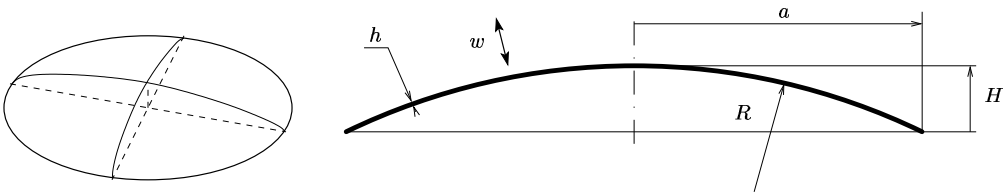

Figure 1: *Geometry of the shell: three-dimensional sketch and cross section.*

2.1 Continuous model and discretization

A spherical shell of thickness h, radius of curvature R and outer diameter $2a$, made of a homogeneous isotropic material of density ρ, Poisson ratio ν and Young's modulus E, is considered. The geometry is specified on Fig.1. The equations of motion, in terms of the transverse displacement w and the Airy stress function F, for all time t, are:

$$D\Delta\Delta w + \frac{1}{R}\Delta F + \rho h\ddot{w} = L(w,F) - c\dot{w} + p, \qquad \Delta\Delta F - \frac{Eh}{R}\Delta w = -\frac{Eh}{2}L(w,w), \tag{1}$$

where D is the flexural rigidity, c is a damping coefficient, p represents the external normal pressure, $\ddot{w}$ is the second partial derivative of w with respect to time, Δ is the Laplacian and L is the usual von Kármán bilinear quadratic operator [2].

In the following, dimensionless equations corresponding to Eqs. (1) are used. The scaling of w is chosen so that $\bar{w} = w/h$. It is the one used in [5] to whom the interested reader can refer for the definition of the other dimensionless variables. One can note that the scaling of time t, $\bar{t} = h/a^2\sqrt{E/12\rho(1-\nu^2)}\,t$ do not depends on the scaling of w. In the following, as any variable is dimensionless, the overbars are dropped.

The transverse deflection is expanded on the eigenmodes of the associated linear problem. The solution is sought as:

$$w(r,\theta,t) = \sum_{p=1}^{+\infty} \Phi_p(r,\theta)\, X_p(t). \tag{2}$$

The $\{X_p\}_{p\in\mathbb{N}^*}$ are unknown functions of time - the modal coordinates - and Φ_p is the p-th mode shape of the shell with free edge, whose analytical expression can be found in [2]. Using the orthogonality property of the $\{\Phi_p\}$, one obtains that the $\{X_p\}$ are the solutions of the following set of non-linear coupled oscillators:

$$\ddot{X}_p + 2\xi_p\omega_p\dot{X}_p + \omega_p^2 X_p + \sum_{i=1}^{+\infty}\sum_{j=1}^{+\infty} g_{ij}^p X_i X_j + \sum_{i=1}^{+\infty}\sum_{j=1}^{+\infty}\sum_{k=1}^{+\infty} h_{ijk}^p X_i X_j X_k = \tilde{Q}_p(t), \tag{3}$$

where (ω_p,ξ_p) are respectively the dimensionless natural frequency and damping factor of mode p. $\{g_{ij}^p\}$ and $\{h_{ijk}^p\}$ are coefficients that depends on the mode shapes and the geometry of the shell. They have been calculated in [2]. One can note that the "small" parameters ε_q and ε_c introduced in [2] are here included in the coefficients, so that $g_{ij}^p = \varepsilon_q\beta_{ij}^p$ and $h_{ijk}^p = \varepsilon_c\Gamma_{ijk}^p$.

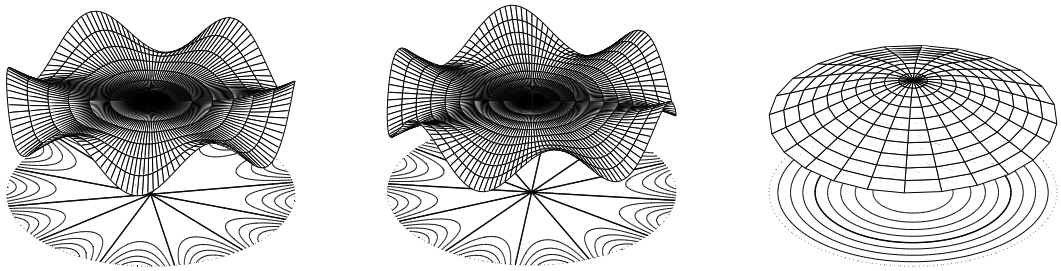

Figure 2: *The three involved mode. From left to right: both mode (6,0) (mode 1 and 2) and mode (0,1) (mode 3).*

2.2 The internal resonance

A particular 1:1:2 internal resonance between two companion purely asymmetric modes (denoted in the following by mode 1 and mode 2) of dimensionless natural frequencies ω_1 and ω_2 and an axisymmetric mode (mode 3) of dimensionless natural frequency ω_3 is now studied (see Fig. 2). This internal resonance occurs if:

$$\omega_3 \simeq 2\omega_1 \simeq 2\omega_2. \tag{4}$$

The two next sections describe two reduced-order models designed to predict the exchanges of energy between the three involved modes and the special vibratory response of the shell that ensue.

2.3 Model A: three linear modes without cubic non-linearities

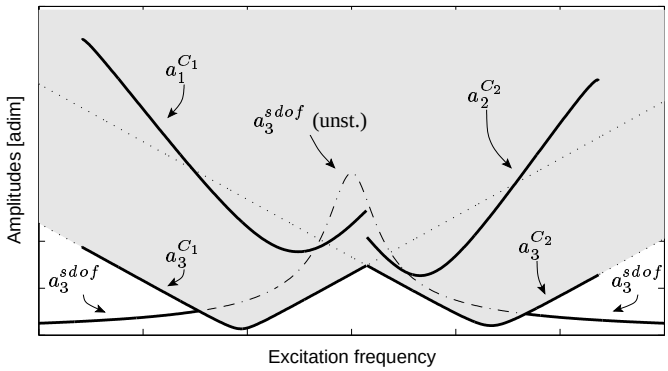

Figure 3: Theoretical frequency response curves.

Model A stems from the simplest truncation of set (3): it consists of retaining only the three oscillators associated to modes 1, 2 and 3 and to neglect the cubic terms. The dimensionless displacement of the shell in steady-state is then:

$$w(r,\theta,t) = \Phi_1(r,\theta)X_1(t) + \Phi_2(r,\theta)X_2(t) + \Phi_3(r)X_3(t), \tag{5}$$

and the $\{X_p\}_{p=1,2,3}$ are solutions of:

$$\ddot{X}_1 + 2\xi_1\omega_1\dot{X}_1 + \omega_1^2 X_1 = \alpha_1 X_1 X_3, \tag{6a}$$

$$\ddot{X}_2 + 2\xi_2\omega_2\dot{X}_2 + \omega_2^2 X_2 = \alpha_2 X_2 X_3, \tag{6b}$$

$$\ddot{X}_3 + 2\xi_3\omega_3\dot{X}_3 + \omega_3^2 X_3 = \alpha_3 X_1^2 + \alpha_4 X_2^2 + Q\cos\Omega t. \tag{6c}$$

In the above set, it has been assumed that the structure is driven at its center by a harmonic forcing of angular frequency Ω and amplitude Q. Since the shapes of modes 1 and 2 have a node at center, the forcing terms in Eqs. (6b,c) vanish.

When the structure is driven in the vicinity of the resonance of mode 3 ($\Omega \simeq \omega_3$), a first order solution to the above set (6a-c) obtained by a perturbation method is:

$$X_1(t) = a_1 \cos\left(\frac{\Omega}{2}t - \frac{\gamma_1+\gamma_3}{2}\right), \quad X_2(t) = a_2 \cos\left(\frac{\Omega}{2}t - \frac{\gamma_2+\gamma_3}{2}\right), \quad X_3(t) = a_3\cos(\Omega t - \gamma_3). \quad (7)$$

The values of the amplitudes $\{a_i\}_{i=1,2,3}$ and phases $\{\gamma_i\}_{i=1,2,3}$, as functions of Ω and Q, have been obtained in [2]. It is shown that only three stable vibratory solutions can be obtained in the steady state:

- the SDOF solution (single-degree-of-freedom), with $a_1 \equiv a_2 \equiv 0$ and $a_3 \neq 0$, which is the usual uncoupled solution;
- the C_1 solution, with $a_1 \neq 0$, $a_2 \equiv 0$, $a_3 \neq 0$: an energy transfer occurs between mode 3 and 1;
- the C_2 solution, with $a_1 \equiv 0$, $a_2 \neq 0$, $a_3 \neq 0$: an energy transfer occurs between mode 3 and 2.

Moreover, in the (a_3, Ω) plane, the SDOF solution is stable outside an instability region, inside whom the coupled solutions C_1 and C_2 take birth. This region is shown with a gray shaded area on Figure 3.

2.4 Comparison to experiments

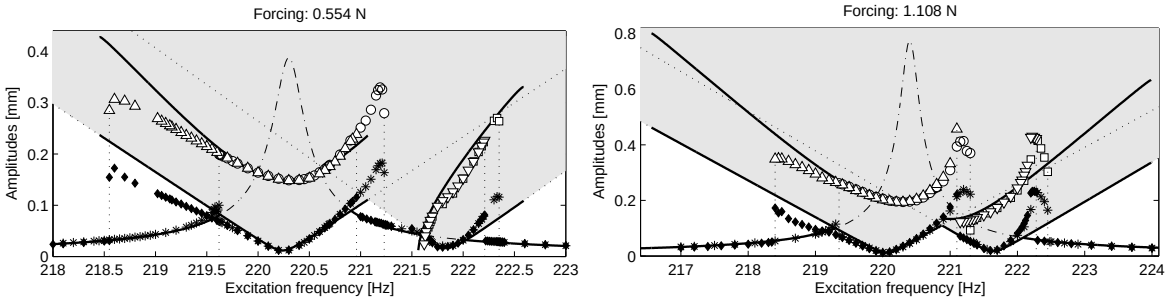

Figure 4: Comparison of experiments to the results of model A. Left: resonance curve for a forcing amplitude of 0.554 N. Right: resonance curves for a forcing amplitude of 1.108 N (from [3]).

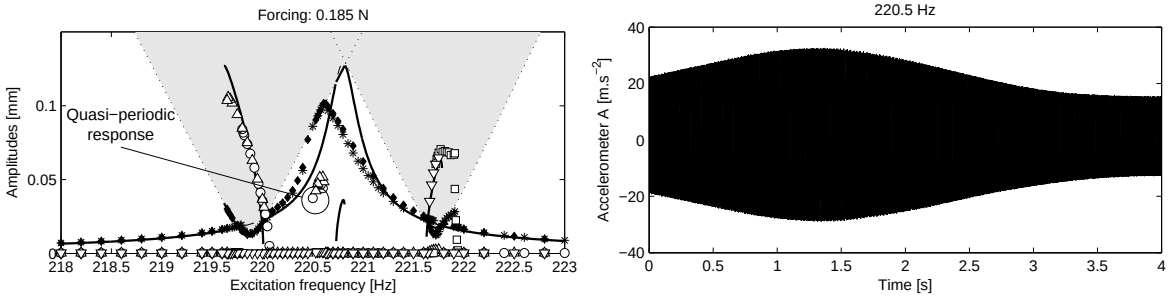

Figure 5: Comparison of experiments to the results of model A. Left: resonance curves for a forcing amplitude of 0.185 N. Right: quasiperiodic response (from [3]).

A special setup has been designed to measure the amplitudes of the three involved modes as well as the boundaries of the instability regions. The interested reader can refer to [3, 7] for details. Figure 4 and 5 show some comparisons between the predictions of model A and the experiments. Even if experiments and theory are in excellent qualitative agreement, the following discrepancies can be noticed.

- For large forcing levels ($F_{dr} = 1.108$ N, Fig. 4, left), the fine geometry of the experimental points is not respected by the theory, as well as the limits of the stability frequency bands of the coupled solutions.

- Some solutions with amplitude modulations have been noticed for some localized frequency bands (see Fig. 5).

- In the experiments, the a_3 branches for the C_1 and C_2 solutions do not coincide with the boundary of the instability region, which is the case for the theory (see Fig. 4, right).

- Some experimental SDOF solution are curved toward the low frequencies, as if they were governed by a softening non-linear behavior. This feature cannot be predicted by model A, which includes only quadratic terms (see Fig. 5).

It was also found that some slight geometrical imperfections of the experimental shell, as compared to a perfect spherical cap, have a major effect on the vibratory response. A consequence is that some experimental frequencies as well as non-linear coefficients $\{\alpha_i\}$ in Eqs (6) are overestimated by theory. As an example, the natural frequency of mode 3 is estimated at 386 Hz and measured at 225 Hz and an overestimation factor of 30 has been found for coefficients $\{\alpha_i\}$ [3].

2.5 Model B: three non-linear normal modes

In order to correct the discrepancies observed between model A and experiments, a more refined model has been built. The leading idea is that the cubing non-linear terms are the main responsible of the discrepancies observed, so an upgraded model should keep these cubic terms so as to recover, *e.g.* the curvature of the SDOF solution, the difference between the position of the coupled a_3 solutions and the instability region and the quasiperiodic regimes found on coupled branches.

However, keeping the cubic terms in the dynamical equations leads to reconsider the modal truncation. Keeping only the linear modes involved in the resonance may produce erroneous results, so that one must a priori keep numerous linear modes to attain convergence. In this context, reducing the system to its Non-linear Normal modes (NNMs) is an efficient procedure for keeping the same number of oscillators, without neglecting others that are enslaved to the chosen master coordinates.

The reduced model used here is built with the following procedure. First, 21 linear modes are kept in the truncation, they are: (2,0) to (9,0) (with preferential $\sin$ and $\cos$ configuration, resulting in 16 modes), axisymmetric modes (0,1) to (0,3), and mixed mode (1,1) with its two configurations. The non-linear coefficients are computed according to the full model derived in [2]. From the subset of 21 non-linear oscillators with quadratic and cubic non-linear terms, the non-linear change of coordinates, allowing to pass from the modal variables to the normal ones, describing the motions in an invariant-based span of the phase space (the NNMs), is processed, following the procedure explained in [6, 8]. The normal form procedure of [6, 8] is an extension of the reduction method proposed in [4], which was limited to conservative cases. The following change of coordinates is applied:

$$\begin{aligned} X_p =& R_p + \sum_{i=1}^{N}\sum_{j\geq i}^{N}(a_{ij}^p R_i R_j + b_{ij}^p S_i S_j) + \sum_{i=1}^{N}\sum_{j=1}^{N} c_{ij}^p R_i S_j + \sum_{i=1}^{N}\sum_{j\geq i}^{N}\sum_{k\geq j}^{N}\left(r_{ijk}^p R_i R_j R_k + s_{ijk}^p S_i S_j S_k\right) \\ &+ \sum_{i=1}^{N}\sum_{j=1}^{N}\sum_{k\geq j}^{N}\left(t_{ijk}^p S_i R_j R_k + u_{ijk}^p R_i S_j S_k\right), \end{aligned} \tag{8a}$$

$$\begin{aligned} Y_p =& S_p + \sum_{i=1}^{N}\sum_{j\geq i}^{N}(\alpha_{ij}^p R_i R_j + \beta_{ij}^p S_i S_j) + \sum_{i=1}^{N}\sum_{j=1}^{N} \gamma_{ij}^p R_i S_j + \sum_{i=1}^{N}\sum_{j\geq i}^{N}\sum_{k\geq j}^{N}\left(\lambda_{ijk}^p R_i R_j R_k + \mu_{ijk}^p S_i S_j S_k\right) \\ &+ \sum_{i=1}^{N}\sum_{j=1}^{N}\sum_{k\geq j}^{N}\left(\nu_{ijk}^p S_i R_j R_k + \zeta_{ijk}^p R_i S_j S_k\right). \end{aligned} \tag{8b}$$

with $N = 21$.

Then the 3 coordinates corresponding to the NNMs that continues the three linear modes: both (6,0) companion modes and (0,1), are selected, the others are set to zero. The reduced dynamics on this 6-dimensional

invariant manifold reads, according to the general case derived in [6, 8]:

$$\ddot{R}_1 + \omega_1^2 R_1 + g_{13}^1 R_1 R_3 + 2\xi_1\omega_1\dot{R}_1 + (A_{111}^1 + h_{111}^1)R_1^3 + B_{111}^1 R_1\dot{R}_1^2 + C_{111}^1 R_1^2\dot{R}_1 + (A_{212}^1 + A_{122}^1 + h_{122}^1)R_1R_2^2 + B_{122}^1 R_1\dot{R}_2^2 + B_{212}^1\dot{R}_1R_1\dot{R}_2 + (C_{122}^1 + C_{212}^1)R_1R_2\dot{R}_2 + C_{221}^1 R_2^2\dot{R}_1 + (A_{313}^1 + A_{133}^1 + h_{133}^1)R_1R_3^2 + B_{133}^1 R_1\dot{R}_3^2 + B_{313}^1\dot{R}_1R_1\dot{R}_3 + (C_{133}^1 + C_{313}^1)R_1R_3\dot{R}_3 + C_{331}^1 R_3^2\dot{R}_1 = 0 \quad (9a)$$

$$\ddot{R}_2 + \omega_2^2 R_2 + g_{23}^2 R_2 R_3 + 2\xi_2\omega_2\dot{R}_2 + (A_{222}^2 + h_{222}^2)R_2^3 + B_{222}^2 R_2\dot{R}_2^2 + C_{222}^2 R_2^2\dot{R}_2 + (A_{112}^2 + A_{211}^1 + h_{112}^1)R_2R_1^2 + B_{211}^2 R_2\dot{R}_1^2 + B_{112}^2\dot{R}_2R_1\dot{R}_1 + (C_{211}^2 + C_{121}^2)R_2R_1\dot{R}_1 + C_{112}^2 R_1^2\dot{R}_2 + (A_{323}^2 + A_{233}^2 + h_{233}^2)R_2R_3^2 + B_{233}^2 R_2\dot{R}_3^2 + B_{323}^2\dot{R}_2R_2\dot{R}_3 + (C_{233}^2 + C_{323}^2)R_2R_3\dot{R}_3 + C_{332}^2 R_3^2\dot{R}_2 = 0 \quad (9b)$$

$$\ddot{R}_3 + \omega_3^2 R_3 + g_{11}^3 R_1^2 + g_{22}^3 R_2^2 + 2\xi_3\omega_3\dot{R}_3 + (A_{333}^3 + h_{333}^3)R_3^3 + B_{333}^3 R_3\dot{R}_3^2 + C_{333}^3 R_3^2\dot{R}_3 + (A_{113}^3 + A_{311}^3 + h_{113}^3)R_3R_1^2 + B_{311}^3 R_3\dot{R}_1^2 + B_{113}^3\dot{R}_3R_1\dot{R}_1 + (C_{311}^3 + C_{131}^3)R_3R_1\dot{R}_1 + C_{113}^3 R_1^2\dot{R}_3 + (A_{223}^3 + A_{322}^3 + h_{223}^3)R_3R_2^2 + B_{322}^3 R_3\dot{R}_2^2 + B_{223}^3\dot{R}_3R_2\dot{R}_2 + (C_{322}^3 + C_{232}^3)R_3R_2\dot{R}_2 + C_{223}^3 R_2^2\dot{R}_3 = Q\cos\Omega t \quad (9c)$$

Then, by using the change of co-ordinates of Eqs. (8), one can obtains the modal co-ordinates $\{X_p\}_{p=1\ldots21}$.

3 COMPARISON BETWEEN MODELS AND EXPERIMENTS

χ [adim]	a [m]	h [m]	R [m]	ρ [kg/m^3]	E [GPa]	ν [adim]
9560	0.3 m	$1\cdot10^{-3}$	3.01	8230	111.44	0.33

	f_1 [Hz]	f_2 [Hz]	f_3 [Hz]	ξ_1 [adim]	ξ_2 [adim]	ξ_3 [adim]	F_{dr} [N]
Case 1 (Fig. 6)	97.8	98.8	195.4	$5\cdot10^{-4}$	$5\cdot10^{-4}$	$5\cdot10^{-4}$	0.039
Case 2 (Fig. 7)	97.8	98.8	195.4	$5\cdot10^{-4}$	$5\cdot10^{-4}$	$5\cdot10^{-4}$	0.081
Case 3 (Fig. 8)	92.1	101.9	195.4	$8\cdot10^{-3}$	$8\cdot10^{-3}$	$4\cdot10^{-3}$	1.07

Table 1: Numerical values of parameters

In this section, numerical solutions of dynamical system (9a-c) are presented, in order to compare model B to model A and experiments. The simulations are obtained with software AUTO, which is capable of solution continuation with the pseudo arc-length method [9].

The value of all parameters used in the simulation of model B are the ones obtained theoretically in [2]. The value of the aspect ratio $\chi = 12(1-\nu^2)a^4/R^2h^2$ of the shell has been chosen so that theoretical natural frequencies precisely fulfills the 1:1:2 internal resonance relationship. The natural frequencies of the companion $(6,0)$ modes are slightly modified compared to the perfect case, in order to obtain coupled solutions qualitatively as closer as possible than those obtained experimentally (see Figs. 4,5). The values of all parameters are gathered in Tab. 1, for the three following simulations.

The forcing level for the first simulation (Case 1, Fig. 6) has been chosen so that the obtained resonance curve is similar to the one of Fig. 4, left. In this case of medium forcing level, one can see that model B gives an additional branch of unstable C_2 solution that connects C_1 and C_2 solutions. The second simulation (Case 2, Fig. 7 to be compared to Fig. 5, right), obtained with the same set of parameters but with a larger forcing level, predicts that a quasi-periodic additional solution replaces an unstable C_2 solution in a small frequency range around 196 Hz. One can note that these amplitude-modulated solutions would be difficult to be observed experimentally since (i) they are not the continuation of stable branches and (ii) a C_2 stable branch exists in the same frequency range. An interesting characteristic of model B is that in both case 1 and case 2, it gives branches of solution with shapes closer to the one obtains experimentally: C_1 and C_2 branches are located respectively below and above the ones obtains with model A, with the same trends than in the experiments (compare Figs. 4, 6(b) and 7(a)).

Finally, for the third simulation (Case 3, Fig. 8), the natural frequencies of modes (6,0) have been changed to fit the experiments of Fig. 5. It is shown that model B predicts quasi-periodic responses that replace C_1 and

C_2 stable solutions obtained by model A in the frequency range around natural frequency f_3 of mode 3. A simulation of the time-evolution of the normal co-ordinates (Fig. 8(b) shows that the period of the amplitude modulation ($\simeq 5$ s) is of the same order than the one obtained experimentally (Fig. 5, right).

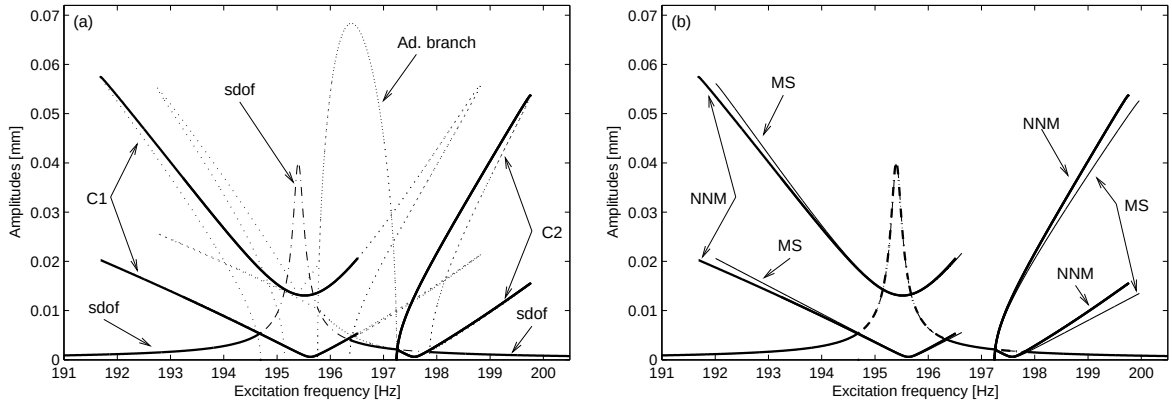

Figure 6: Case 1: comparison between model A (Multiple Scale solution, MS) and model B (NNM) with $F_{dr} = 0.039$ N. '—': stable solutions, '-·-': unstable SDOF solution, '···': other unstable solutions.

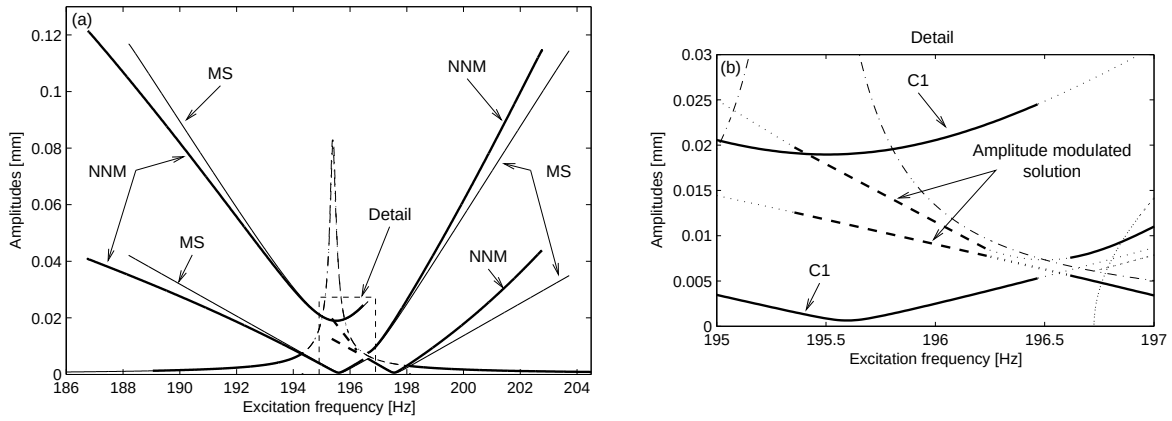

Figure 7: Case 2: comparison between model A (Multiple Scale solution, MS) and model B (NNM) with $F_{dr} = 0.081$ N. '—': stable solutions, '-·-': unstable SDOF solution, '···': other unstable solutions, '- -': quasi-periodic solutions.

4 CONCLUSION

In this article, a special 1:1:2 internal resonance in a shallow spherical shell was addressed. A reduced-order model (denoted as model B), based on three non-linear modes, was built in order to correct some discrepancies previously observed between a simpler model (model A) and experiments. It was shown that model B is qualitatively closer to the experiments than model A. In particular, model B recovers the overall shape of the solutions branches obtained experimentally. Moreover, quasi-periodic solutions are predicted by model B in similar frequency ranges than those observed experimentally.

However, as all parameters (the natural frequencies and the coefficients of non-linear terms) of model B are related to a shell with a perfectly spherical geometry, the drawbacks related to the geometrical imperfections of the experimental shell are not taken into account. In particular, the branches amplitudes obtained with model B are lower (of a factor of 10) than the ones obtained experimentally. This probably explains why other experimental characteristics of the experimental resonance curves are not recovered by model B, namely, the

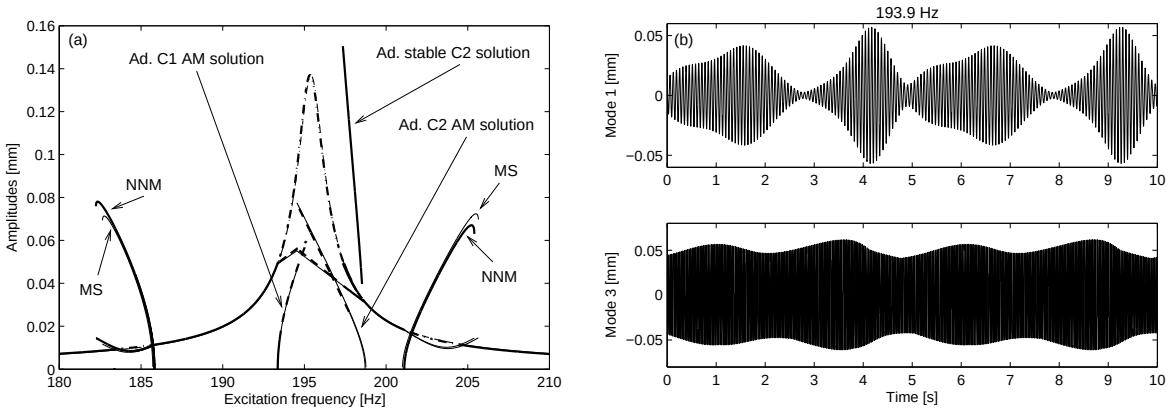

Figure 8: Case 3. (a) comparison between model A (Multiple Scale solution, MS) and model B (NNM); '—': stable solutions, '-·-': unstable SDOF solution, '- -': quasi-periodic solutions. (b) time evolution of R_1 and R_3 for $f_{dr} = 193.9$ Hz.

curvature of the SDOF solution toward the low frequencies and the non-coincidence of the instability region boundaries and mode 3 coupled branches.

References

[1] A. H. Nayfeh. *Nonlinear interactions*. J. Wiley & sons, 2000.

[2] O. Thomas, C. Touzé, and A. Chaigne. Non-linear vibrations of free-edge thin spherical shells: modal interaction rules and 1:1:2 internal resonance. *International Journal of Solids and Structures*, 42(11-12):3339–3373, 2005.

[3] O. Thomas, C. Touzé, and É. Luminais. Non-linear vibrations of free-edge thin spherical shells: experiments on a 1:1:2 internal resonance. *Nonlinear Dynamics*, 2006. Submitted.

[4] C. Touzé, O. Thomas, and A. Chaigne. Hardening/softening behaviour in non-linear oscillations of structural systems using non-linear normal modes. *Journal of Sound and Vibration*, 273(1-2):77–101, 2004.

[5] C. Touzé and O. Thomas. Non-linear behaviour of free-edge shallow spherical shells: effect of the geometry. *International Journal of non-linear Mechanics*, 2005. in press.

[6] C. Touzé and M. Amabili. Non-linear normal modes for damped geometrically non-linear systems: application to reduced-order modeling of harmonically forced structures.

[7] O. Thomas, C. Touzé, and É. Luminais. Non-linear modal interactions in free-edge thin spherical shells: measurements of a 1:1:2 internal resonance. In *Third M.I.T. Conference on Computational Fluid and Solid Mechanics*, Cambridge, USA, June 2005.

[8] C. Touzé, M. Amabili, and O. Thomas. Reduced-order models for damped geometrically non-linear vibrations of thin shells via real normal form. In *2nd International Conference on Nonlinear Normal Modes and Localization in Vibrating Systems*, Karlovasi, Samos, Greece, June 2006.

[9] E. Doedel, R. Paffenroth, A. Champneys, T. Fairgrieve, Y. Kuznetsov, B. Oldeman, B. Sandstede, and X. Wang. Auto 2000: continuation and bifurcation software for ordinary differential equations. Technical report, Concordia University, 2002. *http://indy.cs.concordia.ca/auto*.